



www.cafetinnova.org

Indexed in
Scopus Compendex and Geobase Elsevier, Chemical
Abstract Services-USA, Geo-Ref Information Services-USA,
List B of Scientific Journals, Poland,
Directory of Research Journals

**International Journal
of Earth Sciences
and Engineering**

April 2015, P.P.272-278

ISSN 0974-5904, Volume 08, No. 02

Kinetics Aspects and Dynamic Interaction of Aqueous Cr (III) and Cr (VI) Species with Fired Muthurajawela Peat

N PRIYANTHA^{1,2}, LINDA B L LIM³, S WICKRAMASOORIYA^{1,2}

¹Department of Chemistry, ²Postgraduate Institute of Science, University of Peradeniya, Peradeniya, Sri Lanka

³Department of Chemistry, Universiti Brunei Darussalam, Brunei Darussalam

Email: namalpriyantha@pdn.ac.lk, namal.priyantha@yahoo.com

Abstract: Inexpensive and naturally available substances, such as peat, show beneficial advantages for heavy metal removal from aqueous media, which can be further enhanced through heat treatment. Series of experiments conducted by varying shaking time and settling time individually over a wide range using Muthurajawela peat (MP) fired at 200°C, the pre-determined optimum value, lead to optimized conditions for removal of Cr(VI) of 2.5 h shaking time and 1.0 h settling time while those are 3.0 h and 2.0 h for Cr(III), respectively. Application of kinetics models on the removal of both metal species at different solution temperatures reveals that adsorption of Cr(III) and Cr(VI) species on MP fired at 200°C attains equilibrium through pseudo second order kinetics. Intra-particle diffusion model suggests that the rate limiting step of adsorption of these two species on fired MP has another contribution in addition to intra-particle diffusion, while the homogeneous solid diffusion model suggests that the process is controlled by film diffusion (external diffusion) along with intra-particle diffusion. Diffusivity of the adsorption reaction is increased from $2.23 \times 10^{-9} \text{ m}^2 \text{ min}^{-1}$ to $7.80 \times 10^{-9} \text{ m}^2 \text{ min}^{-1}$ with the increase in the solution temperature from ambient temperature to 60°C, while the change is from $1.00 \times 10^{-9} \text{ m}^2 \text{ min}^{-1}$ to $1.29 \times 10^{-9} \text{ m}^2 \text{ min}^{-1}$ for Cr (VI). The efficiencies of removal of Cr (III) and Cr (VI) on a fixed bed column are approximately 85% and 90%, respectively.

Keywords: peat, kinetics models, chromium, diffusion

1. Introduction

Chromium species, available as $\text{Cr}_2\text{O}_7^{2-}$, CrO_4^{2-} and Cr^{3+} in aqueous systems, are more toxic than other forms. These species are discharged to the environment with industrial activities, such as electroplating, leather tanning and metal finishing [1]. On the other hand, sludge and municipal discharges lead to elevated concentrations of chromium species and other metals in waste water [2]. Consequently, it is a necessity to treat such effluents before discharged to the environment.

Removal of heavy metals and their compounds from wastewater is a necessary requirement for the purification of water in order to fulfill the requirements of the green technology. Reduction, precipitation, ion exchange and reverse osmosis are used as conventional methods for their removal [3]. Recent studies demonstrate that heavy metal removal can effectively be accomplished through adsorption, mainly under batch experimental conditions [4, 5]. In this regard, inexpensive and naturally available substances, such as peat, plant biomass and clay types, become attractive [6-8]. Most of the studies reported on heavy metal removal by peat have utilized its natural form [9, 10]. Different forms of natural peat have exhibited the removal of

heavy metals, while thermally treated brick clay has shown significant removal efficiency of Cr(VI) from aqueous medium [1, 4, 5]. Further, thermally treated Muthurajawela peat (MP) has shown stronger ability to remove Cr(III) and Cr(VI) species than its natural form.

Maximization of removal efficiency within a reasonable period of time, which can be accomplished through optimization of experimental conditions, is a key step in extension of this type research toward applications. On the other hand, information on adsorption provides knowledge on the mode of interaction of the adsorbent with heavy metal ions, which depends on its chemical and physical properties. Hence, the residence time required for adsorption process can be determined using kinetics data. Kinetics studies of Zn(II), Cd(II) and Hg(II) from aqueous solution using zinc oxide nanoparticles has revealed that initial adsorption is controlled by film diffusion, followed by pore diffusion [11]. Adsorption of Cr(VI) on activated carbon has revealed that the system attains equilibrium through pseudo first order kinetics [12]. Various adsorbents, such as citrus peels, green manufactured nano particles, wheat shell and modified agricultural waste, have been used to study the kinetics of removal of metal ions, such

as Cu(II), Cr(VI) and Cd(II), to investigate the sorption mechanism on its surfaces [13-16].

Adsorption kinetics of Cr(III) and Cr(VI) on fired MP at different solution temperatures has not been reported. Such studies would be important to investigate the feasibility of development of low-cost dynamic systems for the reduction of Cr(VI) to sufficiently low levels to meet the regulatory guidelines. In this context, differences of kinetics in batch systems at different solution temperatures for adsorption, and variation of the extent of removal of Cr(III) and Cr(VI) under dynamic conditions with respect to flow rate and column height were investigated.

2. Materials and Methods

2.1. Materials, Sample Preparation and Instrumentation

Representative peat samples obtained from Muthurajawela, Sri Lanka, was ground well to obtain particles of diameter $1 \text{ mm} < d < 2 \text{ mm}$, manually homogenized and fired at $200 \text{ }^\circ\text{C}$. Analytical grade $\text{K}_2\text{Cr}_2\text{O}_7$ (BDH Chemicals) and $\text{Cr}(\text{NO})_3$ were used to prepare standard solutions in distilled water. The Carbolite CTF 12/100/900 furnace was used to fire MP samples, while metal ion concentrations were determined using Spectro-Electronic M Series atomic absorption spectrophotometer (AAS). SEM images were obtained from Tescan Vega XMU Scanning Electron Microscope (SEM).

2.2. Investigation of Kinetics

Kinetics models, such as pseudo second order, intra-particle diffusion and Elovich Equation, were tested for the removal of Cr(III) and Cr(VI) on peat fired at $200 \text{ }^\circ\text{C}$. For kinetics studies, aliquots of 600 cm^3 solutions of Cr(III) and Cr(VI) each of 10.0 mg L^{-1} concentration were treated with 60.0 g of peat fired at $200 \text{ }^\circ\text{C}$. While the solution was being stirred, 10.00 cm^3 aliquots of the solution were withdrawn at every one minute interval up to 20 min. Then, samples were withdrawn at 10.0 min time intervals until equilibrium was reached at 1.0 h.

2.3. Dynamic Studies

Removal efficiency of Cr(III) and Cr(VI) was measured under different flow rates and different column heights ($d = 2.0 \text{ cm}$) for 10.0 mg L^{-1} Cr(III) or Cr(VI) solution using MP particles ($1 \text{ mm} < d < 2 \text{ mm}$). Samples were withdrawn at every 10.0 min interval and the efficiency of removal was calculated using Equation (1).

$$\text{Percentage removal} = \frac{(C_0 - C_t)}{C_0} \times 100 \quad (1)$$

where C_0 (mg L^{-1}) and C_t (mg L^{-1}) are the inflow concentration and the outflow concentration, respectively, of the metal ion.

3. Theory: Mathematical Modeling

3.1. Pseudo Second Order (PSO)

The transient adsorption in a liquid/solid system is described by the pseudo second order kinetics model. The rate of adsorption can be determined by the rate constant related to this model. In this model, rate of adsorption is proportional to the square of unoccupied sites, as shown in Equation (2),

$$\frac{dq_t}{dt} = k (q_e - q_t)^2 \quad (2)$$

where t is contact time, q_e is the amount of metal ions sorbed from solution (mg kg^{-1}) at equilibrium, q_t is the mass of metals sorbed by unit mass of sorbent at time t and k is the apparent rate constant. As q_t is more conveniently expressed in mg of Cr(III) or Cr(VI) sorbed by 1.0 g of peat fired at $200 \text{ }^\circ\text{C}$, k is estimated in $\text{g mg}^{-1} \text{ min}^{-1}$ for pseudo second order reactions. The analytical solution for Equation (2) is obtained by integrating it followed by the application of suitable boundary conditions to result in Equation (3) [17].

$$\frac{t}{q_t} = \frac{1}{q_e} t + \frac{1}{k q_e^2} \quad (3)$$

3.2. Intra-particle Diffusion (Webber-Morris Model) (IDWM)

The Weber-Morris model states that solute uptake on adsorbent is proportional to the square root of time as shown in Equation (4).

$$q_t = k' t^{0.5} \quad (4)$$

where k' is intraparticle diffusion rate. According to Equation (4), a plot of q_t vs $t^{0.5}$ should be a straight line with a slope of k' when the intra-particle diffusion is the rate-limiting step. This model would not be valid if adsorption kinetics is controlled by film diffusion and intra-particle diffusion simultaneously [18].

3.3. Homogeneous solid diffusion model (HSDM)

Mass transfer in an amorphous and homogeneous sphere is described by this diffusion model, which is represented by,

$$\frac{\partial q}{\partial t} = \frac{D_s}{r^2} \frac{\partial}{\partial r} \left(r^2 \frac{\partial q}{\partial r} \right) \quad (5)$$

The solution of Equation (5) for a data set gathered within a relatively short period of time leads to Equation (6). Since the assumption used to obtain Equation (6) does not satisfy longer time duration, this equation is used only for short time periods [18].

$$\ln \left(\frac{q_e - q_t}{q_e} \right) = \ln \left(\frac{6}{\pi^2} \right) - \frac{\pi^2 D_i}{R^2} t \quad (6)$$

In Equation (5), D_i is the intra-particle diffusion constant ($\text{m}^2 \text{min}^{-1}$) and R is the average radius of an adsorbent particle (m).

If the plot of Equation (6) is linear and passes through the origin, then the actual slowest step in the adsorption process is the intra-particle (internal) diffusion. If not, the process is controlled by film diffusion along with intra-particle diffusion [16].

3.4. Shrinking Core Model (SCM)

This kinetics model has been developed to estimate mass transfer characteristics in the adsorption process. The overall adsorption rate of binding of the adsorbate on the adsorbent (diffusion plus reaction) depends primarily on diffusivity [16]. Variation of the extent of adsorption of chromium species on peat as a function of time is given by Equation (7),

$$(X) = 1 - 3(1 - X)^{\frac{3}{2}} + 2(1 - X) = \frac{6D}{R^2 C^0} \alpha \quad (7)$$

Where

$$X = \frac{C_0 - C_t}{C_0 - C_{eq}} \quad (8)$$

$$\alpha = \int_0^t C_t dt \quad (9)$$

D is the diffusion coefficient ($\text{m}^2 \text{min}^{-1}$), C^0 is the average metal ion binding site density (mg L^{-1}), C_0 and C_t are the initial and final concentration (mg L^{-1}), and C_{eq} is the concentration of solution (mg L^{-1}) at equilibrium.

3.5. Elovich Equation (EE)

Elovich equation is involved with chemisorption. It can be applied for a system which has low desorption rate or no desorption. This is another rate equation based on the retention capacity, which is usually written as follows [17],

$$\frac{dq_t}{dt} = V_0 \cdot e^{-\beta q_t} \quad (10)$$

where V_0 ($\text{mg g}^{-1} \text{min}^{-1}$) is the initial retention rate because $(dq_t/dt) \rightarrow V_0$ as $q_t \rightarrow 0$, and β (g mg^{-1}) is the desorption constant. The original equation is simplified by assuming $V_0 \beta t \gg 1$ [17]. Applying boundary conditions of $q_t = 0$ at $t = 0$ and $q_t = q_t$ at $t = t$, the integrated form of leads to Equation (11),

$$q_t = \frac{1}{\beta} \ln(t) + \frac{1}{\beta} \ln(V_0 \beta) \quad (11)$$

Adsorption, film diffusion and intra-particle diffusion are illustrated in Figure 1.

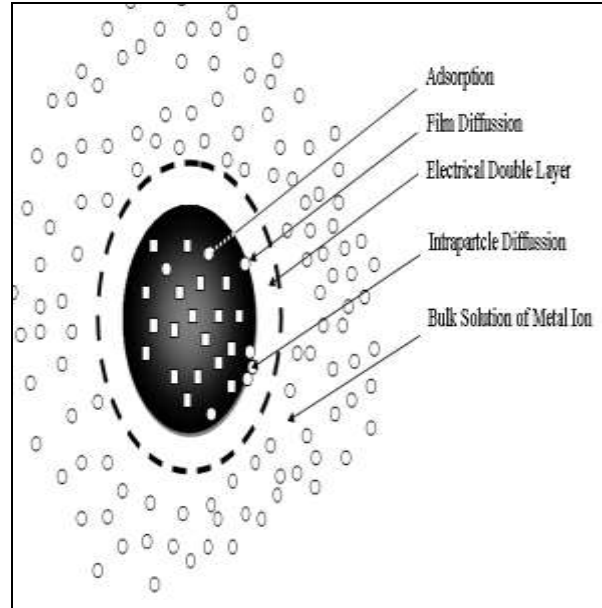


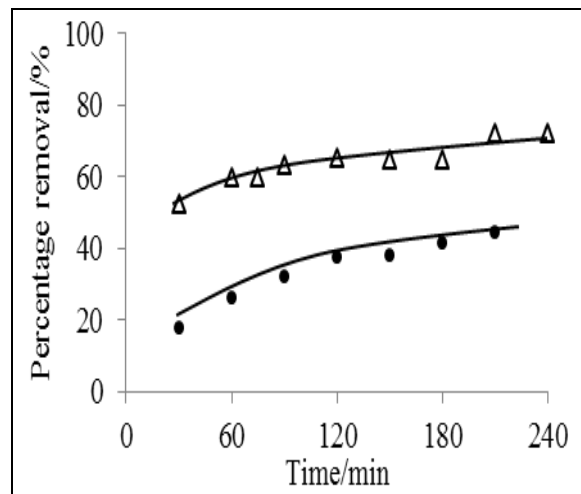
Figure 1 Different model of adsorbent-adsorbate interaction (\circ adsorbate species; \square adsorbent sites) [16]

4. Results and Discussion

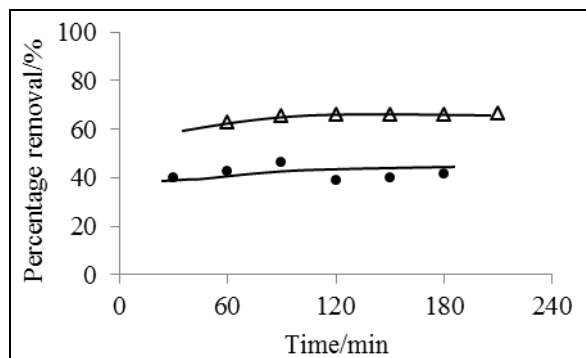
4.1. Kinetics Analysis

The extent of removal of Cr(III) and Cr(VI), determined by treatment of each metal ion solution at ambient pH, for different shaking and settling times, are shown in Figure 2.

Shaking time and settling time of the interaction of Cr(III) or Cr(VI) with MP fired at 200°C were optimized in order to study the removal efficiency. Optimized conditions for removal of Cr(VI) by peat fired at 200°C are determined from the results of Figure 2 are 2.5 h shaking time and 1.0 h settling time, while those are 3.0 h and 2.0 h for Cr(III), respectively.



(a)



(b)

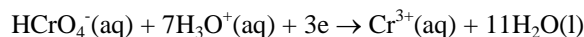
Figure 2 Variation of extent of removal of Cr(III) (●) and Cr(VI) (▲) on MP fired at 200 °C with shaking time (A) and settling time (B). [5.0 g MP ($d < 1\text{mm}$), 10.0 mg L^{-1} of 50.0 cm^3 solution, 3.0 h shaking, 0.5 h settling time].

Kinetics performance of an adsorbent gives the basic idea for a pilot application and the scale of an adsorption process. Adsorption kinetics, in general, is the foundation to determine the performance of fixed-bed or flow-through systems. Once the set of conditions is properly optimized, the extent of sorption leads to the maximum efficiency within a reasonable period of time. Hence, kinetics studies were carried out for the removal of both Cr(III) and Cr(VI) by peat fired at 200 °C in order to identify the mechanism of removal at different solution temperatures. The rate constants were calculated using the PSO kinetics model, while the rate controlling step was subsequently determined by the IDWM model, and the results obtained are listed in Table 1. These models were successfully applied in adsorption of Cr(VI) on fired brick clay [4] and that of Zn(II), Cd(II) and Hg(II) from aqueous solution on zinc oxide nanoparticles [5]. High regression coefficients of the pseudo second order model for Cr(III) and Cr(VI) species on peat fired at 200 °C at different solution temperatures indicate the reasonable validation of the model. Among the three solution temperatures attempted for Cr(III), the best fit ($R^2 = 0.992$) is observed for 60 °C while that for Cr(VI) is ambient temperature ($R^2 = 0.969$). Nevertheless, decrease in the rate constant according to the PSO model cannot be explained using basic principles. The observation of the increase in the diffusion rate constant with the increase in solution temperature according to the IDWM model

is in agreement with kinetic principles. The increase in the extent of removal of Cr(III) with the solution temperature, as observed experimentally, can be explained using the Elovich Equation, whose results listed in Table 1 indicate that the decrease in desorption constant (β) from 125 (g mg^{-1}) to 67 (g mg^{-1}) with solution temperature of Cr(III). It is also clear that the higher adsorption affinity of Cr(III) at 60 °C is more favorable than that of Cr(VI).

Intra-particle diffusion model, which is derived by Webber and Morris (IDWM) provides information on the rate determining step of the adsorption process. However, resulting graphs obtained for the IDWM model does not go through the origin, suggesting that the rate limiting step has another contribution in addition to intra-particle diffusion.

The HSDM model is applied to the systems by assuming that MP has amorphous and homogeneous surface in order to check the effect of surface behavior on adsorption. The SCM model is used to identify kinetics of a system though the film diffusion occurs together with intra-particle diffusion. Linear equation of the HSDM model does not pass through the origin indicating that the process is controlled by film diffusion (external diffusion) along with intra-particle diffusion. According to the SCM model, diffusion constants for the process decrease with increase in solution temperature for both metal ions, which is probably due to changes in the homogeneous surface of MP. Carboxylic and phenolic groups presents in MP may affect these surface changes with solution temperature. Diffusivity (diffusion plus reaction) of the process determined from the SCM model clearly shows that the diffusivity of the Cr(III) is increased from $2.23 \times 10^{-9} \text{ m}^2 \text{ min}^{-1}$ to $7.80 \times 10^{-9} \text{ m}^2 \text{ min}^{-1}$ with the solution temperature. Such a behavior is not encountered for Cr(VI). This may be due to the reduction of Cr(VI) which is present as HCrO_4^- as shown in the following equation.



This difference may be due to the reduction of Cr(VI) leading to increased Cr(III) concentration in solution. Similar diffusivity values have been reported for adsorption of Cu(II) on modified agricultural waste [3].

Table 1 Comparison of kinetics model parameters at different solution temperatures

Kinetics model	Metal ion	Cr(III)			Cr(VI)		
	Solution temperature (°C)	Ambient	45	60	Ambient	45	60
PSO	R^2	0.955	0.913	0.992	0.969	0.869	0.964
	k ($\text{g mg}^{-1} \text{ min}^{-1}$)	4.75	4.99	4.01	3.04	2.03	3.00
IDWM	R^2	0.977	0.866	0.962	0.952	0.932	0.988

	$k'(\text{mg g}^{-1} \text{min}^{-0.5})$	0.006	0.007	0.011	0.010	0.010	0.013
EE	R^2	0.898	0.777	0.962	0.952	0.806	0.925
	$\beta(\text{g mg}^{-1})$	125	125	67	83	77	77
	$V_0(\text{mg g}^{-1} \text{min}^{-1})$	0.02	0.06	0.07	0.03	0.03	0.04
HSDM	R^2	0.937	0.755	0.981	0.978	0.892	0.991
	$D_i(\text{g mg}^{-1} \text{min}^{-1}) \times 10^8$	7.90	5.88	1.12	2.64	2.26	2.07
SCM	R^2	0.937	0.872	0.915	0.625	0.788	0.941
	$D(\text{m}^2 \text{min}^{-1}) \times 10^9$	2.23	2.23	7.80	1.00	1.47	1.29

4.2. Scanning Electron Microscopic (SEM) Analysis

Scanning electron microscopic (SEM) images provide details of surface behavior with respect to surface changes before and after treatment of MP. SEM images of powdered peat samples fired at 200 °C shows the absence of particle nature which are present in unfired peat (Figure 3). This clearly indicates surface changes of peat with firing. The SEM image of Cr(VI)-treated with peat fired at 200 °C shows some surface particles different from the original peat samples. Similarly, SEM images of Cr(III)-treated with peat fired at 200 °C shows a different surface image with respect to Cr(VI). Adsorption of chromium species on peat surfaces is thus confirmed.

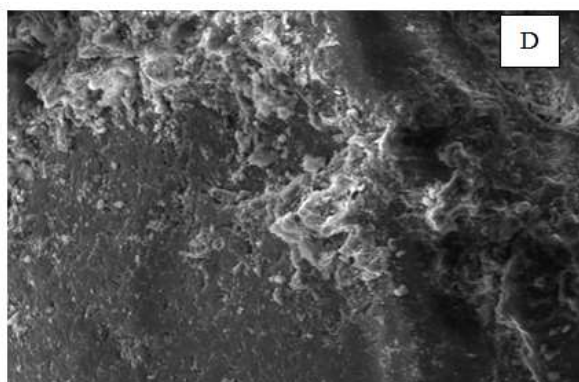
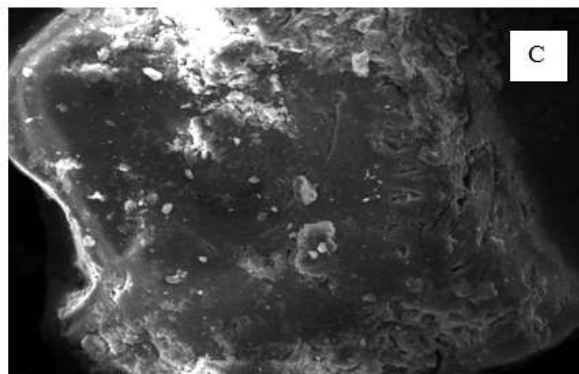
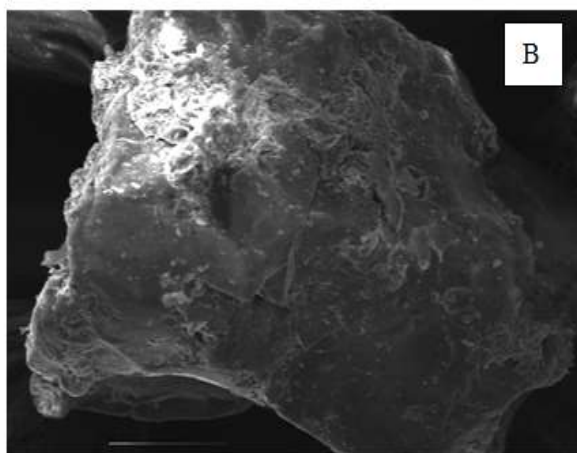
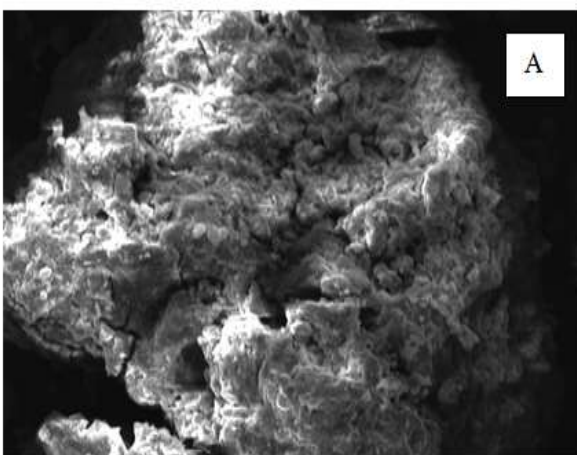


Figure 3 SEM images of MP (A), MP fired at 200 °C (B), followed by treatment with Cr(VI) (C) and Cr(III) (D) (5.00 g peat, 50.0 cm³ solution, optimized shaking and settling time, 1000 mg L⁻¹).

4.3. Removal of Cr(III) and Cu(II) under dynamic condition

The adsorption capacity of the adsorbent obtained from batch equilibrium experiments is useful to provide fundamental information about the effectiveness of a metal sorbent. However, this data would not be applicable to most treatment systems because the contact time would not be sufficient to attain the equilibrium. A packed bed column is an effective process for continuous wastewater treatment, because the concentration difference provides a driving force for heavy metal adsorption. Utilization of adsorbent capacity is results in better quality of the effluent in the dynamic experiments.

Flow rate and the column bed height are important parameters which control the adsorption capacity of a dynamic system. Figure 4 shows the variation of removal efficiency of Cr(VI) with different flow rates from $1.5 \text{ cm}^3 \text{ min}^{-1}$ to $16.0 \text{ cm}^3 \text{ min}^{-1}$ and Figure 5 shows that of for different column heights.

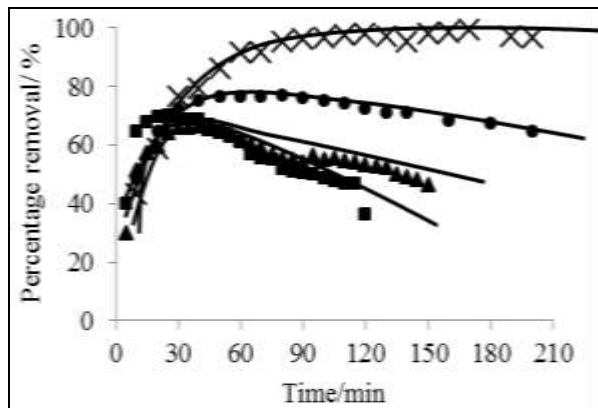


Figure 4 Removal efficiency of Cr(VI) by MP fired at 200°C at different flow rates: $1.5 \text{ cm}^3 \text{ min}^{-1}$ (-x-), $5.0 \text{ cm}^3 \text{ min}^{-1}$ (-●-), $12.0 \text{ cm}^3 \text{ min}^{-1}$ (-▲-) and $16.0 \text{ cm}^3 \text{ min}^{-1}$ (-■-): (height of column = 10.0 cm , i.d. = 2.0 cm , mass of adsorbent = 17.5 g).

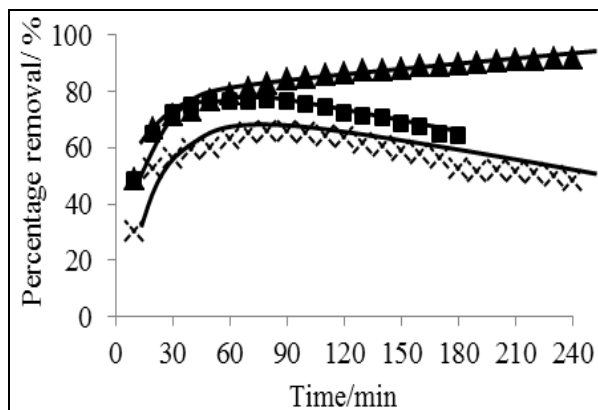


Figure 5 Removal efficiency of Cr(VI) by MP fired at 200°C at a flow rate of $5.0 \text{ cm}^3 \text{ min}^{-1}$ with different column heights: 5.0 cm (-x-), 10.0 cm (-■-) and 20.0 cm (-▲-) [i.d. = 2.0 cm]

Removal efficiency is increased from 60% to 90% with decrease in flow rates while it exhibits 60% to 85% increment along with column height as depicted by Figure 3 and Figure 4, respectively. This would be due to the lower turbulence which boosts adsorbate/adsorbent interactions and availability of more adsorption sites. Weaker interaction and intra-particle mass transfer between the adsorbate molecules and the adsorbent also affect this process.

Figure 6 shows the removal efficiency Cr(III) at different conditions of flow rate and column height.

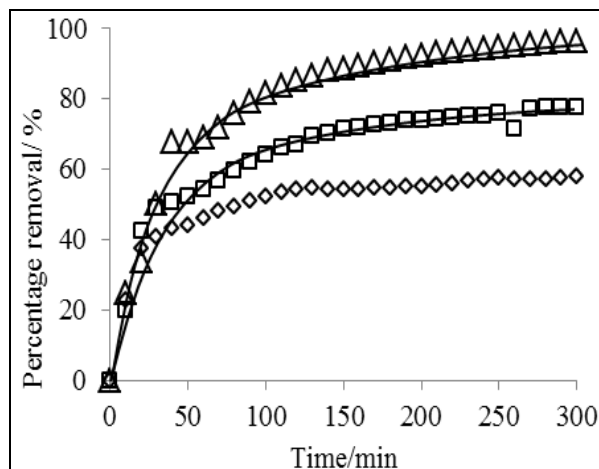


Figure 6 Removal of Cr(III) under dynamic condition with respect to column height 10.0 cm , flow rate $5.0 \text{ cm}^3 \text{ min}^{-1}$ (\diamond), column height 10.0 cm , flow rate $2.5 \text{ cm}^3 \text{ min}^{-1}$ (\square), column height 20.0 cm , flow rate $2.5 \text{ cm}^3 \text{ min}^{-1}$ (Δ).

The maximum extent of removal of Cr(III) in dynamic systems is determined to be 85% for a column with 20.0 cm packing at a flow rate of $2.5 \text{ cm}^3 \text{ min}^{-1}$ after 2.0 h contact time. Further, removal efficiency of Cr(VI) is shown to be greater than Cr(III) with respect to both batch and dynamics conditions. Further, the efficiency can be further increased by changing the amount of adsorbents and flow rate in order to apply to a real treatment system.

5. Conclusion

Optimized conditions for removal of Cr(VI) by peat fired at 200°C are 2.5 h shaking time and 1.0 h settling time, while those are 3.0 h and 2.0 h for Cr(III), respectively. Adsorption process of Cr(VI) and Cr(III) on peat fired at 200°C attains equilibrium through pseudo second order kinetics. Intra-particle diffusion model (IDWM) suggests that the rate limiting step has another contribution in addition to intra-particle diffusion for removal of both metal species. Homogeneous Solid Diffusion Model (HSDM) suggests that the process is controlled by film diffusion (external diffusion) along with intra-particle diffusion. Diffusivity (diffusion plus reaction) of the Cr(III) adsorption process is increased from $2.23 \times 10^{-9} \text{ m}^2 \text{ min}^{-1}$ to $7.80 \times 10^{-9} \text{ m}^2 \text{ min}^{-1}$ with the increase in solution temperature from ambient to 60°C , while it increases from 1.00×10^{-9} to 1.29×10^{-9} for Cr(VI). The efficiency of removal of Cr(III) and Cr(VI) on a fixed bed column (internal diameter = 2.0 cm , particle size of packing = $1.0 - 2.0 \text{ mm}$) is approximately 85% and 90%, respectively, demonstrating the maximum efficiency within the conditions employed. The extent of removal is also affected by the height of column packing, as expected.

Acknowledgement

The authors wish to thank the National Science Foundation of Sri Lanka for providing research grant (RG/2012/BS/02).

References

- [1] D.C. Sharma and C.F. Forster, "Column studies into the adsorption of Chromium(VI) using sphagnum moss peat", *Biosource Technology*, 52., 261-267., 1995.
- [2] S.E. Manahan, *Environmental Chemistry*, 7th edition, Lewis Publishers, Washington., 1990.
- [3] S.S. Baral, N. Das, T.S. Ramulu, S.K. Sahoo and G.R. Chaudhury, "Removal of Cr(VI) by thermally activated weed *Salvinia cucullata* in a fixed-bed column", *Journal of Hazardous Materials*, 161., 1427-1435., 2009.
- [4] L. Zhi-rong, and Z. Li-min, "Competitive adsorption of heavy metal ions on peat", *Journal of China University of Mining*, 18., 0255-0260., 2008.
- [5] X. Cheng, T. Gosset and R. Daniel, "Batch copper ion binding and exchange properties of peat", *Water Research*, 24.12., 1463-1471., 1990.
- [6] N. Priyantha and A. Bandaranayaka, "Investigation of kinetics of Cr(VI)-fired brick clay interaction", *Environmental Science and Pollution Research*, 18., 75-81., 2011.
- [7] N. Priyantha and A. Bandaranayaka, "Interaction of Cr(VI) species with thermally treated brick clay", *Journal of Hazardous Materials*, 188., 193-197., 2011.
- [8] R. Vimala, D. Charumathi and N. Das, "Packed bed column studies on Cd(II) removal from industrial wastewater by macrofungus *Pleurotus platypus*", *Desalination*, 75., 291-296., 2012.
- [9] D. Bog, Gondar, R. Lopez, S. Fiol, J.M. Antelo and F. Arce, "Characterization and acid-base properties of fulvic and humic acids isolated from two horizons of an ombrotrophic peat bog", *Geoderma*, 126., 367-374., 2005.
- [10] F. Qin, B. Wen, X. Shan, Y. Xie, T. Liu, S. Zhang and S.U. Khan, "Mechanisms of competitive adsorption of Pb, Cu, and Cd on peat", *Environmental Pollution*, 144., 669-680., 2006.
- [11] T. Sheela, Y.A. Nayaka, R. Viswanatha, S. Basavanna and T.G. Venkatesha, "Kinetics and thermodynamics studies on the adsorption of Zn(II), Cd(II) and Hg(II) from aqueous solution using zinc oxide nanoparticles", *Powder Technology*, 217., 163-170., 2012.
- [12] M. Barkat, D. Nibou, S. Chegrouche and A. Mellah, "Kinetics and thermodynamics studies of chromium(VI) ions adsorption onto activated carbon from aqueous solutions", *Chemical Engineering and Processing*, 48., 38-47., 2009.
- [13] A. Chatterjee and S. Schiewer, "Multi-resistance kinetic models for biosorption of Cd by rawand immobilized citrus peels in batch and packed-bed columns", *Chemical Engineering Journal*, 244, 105-116., 2014.
- [14] Y. Tu, C. You and C. Chang, "Kinetics and thermodynamics of adsorption for Cd on green manufactured nano-particles", *Journal of Hazardous Materials*, 235-236, 116-122., 2012.
- [15] Y. Bulut and H. Aydın, "A kinetics and thermodynamics study of methylene blue adsorption on wheat shells", *Desalination*, 194., 259-267., 2006.
- [16] S. Kumar, C. Senthamarai and A. Durgadevi, "Adsorption Kinetics, Mechanism, Isotherm, and Thermodynamic Analysis of Copper Ions onto the Surface Modified Agricultural Waste", *Environmental Progress & Sustainable Energy*, 33.1., 2012.
- [17] A. Ronda, M.A. Martin-Lara, M. Calero and G. Blazquez, "Analysis of the kinetics of lead biosorption using native and chemically treated olive tree pruning", *Ecological Engineering*, 58., 278-285., 2013.
- [18] Q. Hui, L. Lu, P. Bing-cai, Z. Qing-jian, Z. Wei-ming and Z. Quan-xing, "Critical review in adsorption kinetic models", *Journal of Zhejiang University Science A*, 10.5., 716-724., 2009.